Available online at www.sciencedirect.com

ScienceDirect

Geochimica et Cosmochimica Acta 125 (2014) 476–491

Geochimica et Cosmochimica Acta

www.elsevier.com/locate/gca

In situ produced branched glycerol dialkyl glycerol tetraethers in suspended particulate matter from the Yenisei River, Eastern Siberia ☆

Cindy De Jonge [a,*], Alina Stadnitskaia [a], Ellen C. Hopmans [a], Georgy Cherkashov [b], Andrey Fedotov [c], Jaap S. Sinninghe Damsté [a]

[a] *Department of Marine Organic Biogeochemistry, NIOZ Royal Netherlands Institute for Sea Research, PO Box 59, 1790 AB Den Burg (Texel), The Netherlands*

[b] *All-Russian Research Institute for Geology and Mineral Resources of the World Ocean (VNIIOkeangeologia), Ministry of Natural Resources, Russian Academy of Science, St. Petersburg, Russian Federation*

[c] *Limnological Institute, Siberian Branch of the Russian Academy of Sciences, Irkutsk, Russian Federation*

Received 10 May 2013; accepted in revised form 18 October 2013; available online 1 November 2013

Abstract

Soil-derived branched glycerol dialkyl glycerol tetraethers (brGDGTs) in marine river fan sediments have a potential use for determining changes in the mean annual temperature (MAT) and pH of the river watershed soils. Prior to their incorporation in marine sediments, the compounds are transported to the marine system by rivers. However, emerging evidence suggests that the brGDGTs in freshwater systems can be derived from both soil run-off and in situ production. The production of brGDGTs in the river system can complicate the interpretation of the brGDGT signal delivered to the marine system. Therefore, we studied the distribution of brGDGT lipids in suspended particulate matter (SPM) of the Yenisei River. Chromatographic improvements allowed quantification of the recently described hexamethylated brGDGT isomer, characterized by having two methyl groups at the 6/6′ instead of the 5/5′ positions, in an environmental dataset for the first time. This novel compound was the most abundant brGDGT in SPM from the Yenisei. Its fractional abundance correlated well with that of the 6-methyl isomer of the hexamethylated brGDGT that contains one cyclopentane moiety. The Yenisei River watershed is characterized by large differences in MAT (>11 °C) as it spans a large latitudinal range (46–73°N), which would be expected to be reflected in brGDGT distributions of its soils. However, the brGDGT distributions in its SPM show little variation. Furthermore, the reconstructed pH values are high compared to the watershed soil pH. We, therefore, hypothesize that the brGDGTs in the Yenisei River SPM are predominantly produced in situ and not primarily derived from erosion of soil. This accounts for the absence of a change in the temperature signal, as the river water temperature is more stable. Using a lake calibration, the reconstructed temperature values agree with the mean summer temperatures (MST) recorded. The brGDGTs delivered to the sea by the Yenisei River during this season are thus not soil-derived, possibly complicating the use of brGDGTs in marine sediments for palaeoclimate reconstructions.

1. INTRODUCTION

Branched glycerol dialkyl glycerol tetraethers (brGDGTs) are ubiquitous membrane lipids in peat and soils. They are derived from bacteria and possess 4–6 methyl substituents ('branches') on the linear C_{28} alkyl chains and up to two cyclopentyl moieties formed by internal cyclization (Fig. 1;

* Corresponding author. Tel.: +31 222369562.
E-mail address: cindy.de.jonge@nioz.nl (C. De Jonge).

0016-7037/$ - see front matter © 2013 The Authors. Published by Elsevier Ltd. All rights reserved.
http://dx.doi.org/10.1016/j.gca.2013.10.031

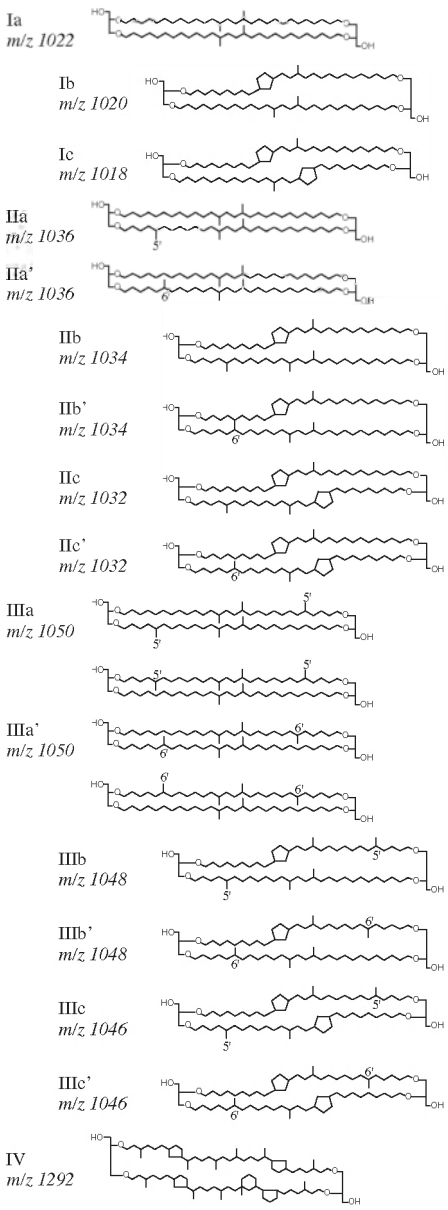

Fig. 1. Chemical structures of branched GDGTs (I–III) and crenarchaeol (IV). The chemical structures of the penta- and hexamethylated brGDGTs with cyclopentyl moiety(ies) IIb′, IIc′, IIIb′ and IIIc′ are tentatively assigned.

Sinninghe Damsté et al., 2000; Weijers et al., 2006a). The distribution of the different brGDGTs depends on the prevailing mean annual temperature (MAT) and soil pH (Weijers et al., 2007). With decreasing temperature, the number of methyl groups in the alkyl chains increase and with a higher soil pH the prevalence of the cyclopentyl moieties will increase. A global soil calibration is thus based on the methylation of branched tetraethers (MBT) and cyclisation of branched tetraethers (CBT) ratios (Weijers et al., 2007). This calibration was recently extended by Peterse et al. (2012), proposing a modified MBT ratio, the MBT′.

Branched GDGTs have also been found in coastal marine sediments, where they are likely deposited by rivers, after erosion and transport of soil particles (Hopmans et al., 2004). The amounts of soil-derived bacterial brGDGTs and the marine Thaumarchaeotal isoprenoid GDGT (iGDGT) crenarchaeol (Sinninghe Damsté et al., 2002) can be expressed in the branched isoprenoid tetraether (BIT) index, which has been used to estimate the amount of soil-derived material in aquatic environments (Hopmans et al., 2004). Furthermore, the distribution of soil-derived brGDGTs in river fan sediments can be used to reconstruct the continental MAT and soil pH of the watershed of the river and this principle has been successfully used for palaeoclimate reconstructions (Weijers et al., 2007). However, complications can arise if the watershed is affected by changes in the supply of organic matter and the source area of the sediments (Bendle et al., 2010). Furthermore, overestimations of MAT have been reported (Schouten et al., 2008; Donders et al., 2009). Recently, structural isomers that partially co-elute with the brGDGTs that are used for these proxy calculations have been described (De Jonge et al., 2013; IIa, IIa′, IIIa, IIIa′; Fig. 1). The abundance and variability of these isomers in the environment is currently unknown, as is their impact on MAT and pH reconstructions based on CBT/MBT indices.

BrGDGTs also occur ubiquitously in lake sediments (e.g. Blaga et al., 2009, 2010) and, since they were thought to be derived from erosion of surrounding soils, the sedimentary record of the BIT index has been applied as an indicator of past variations in the intensity of rainfall in an equatorial lake (Verschuren et al., 2009). The CBT/MBT indices of sedimentary brGDGTs have subsequently also been applied to a variety of lakes, to reconstruct local MAT and pH changes in their watershed (e.g. Tierney et al., 2010, 2012; Niemann et al., 2012; Wang et al., 2012). However, in these studies the CBT/MBT-inferred temperatures using soil-based calibrations often considerably underestimated MAT. The discrepancy between soil and lake brGDGT distributions points to potential in situ production of brGDGTs in lakes (Tierney and Russell, 2009; Sinninghe Damsté et al., 2009; Loomis et al., 2011). Since the prevailing lake temperature still controls the distributions of the brGDGTs in the surface sediments of the lakes this has led to alternative (aquatic) calibrations being created (Tierney et al., 2010; Pearson et al., 2011; Sun et al., 2011; Loomis et al., 2012).

Although rivers are the main pathway for the transport of brGDGTs to ocean sediments, there is a remarkable lack of studies that assess the potential effect of in situ production in rivers. The occurrence of branched GDGTs and crenarchaeol has been reported in suspended particulate material (SPM) from the European Rivers Rhine, Meuse, Niers, and Berkel (Herfort et al., 2006) as well as in the Têt and Rhone Rivers in France (Kim et al., 2007). BrGDGTs have also been shown to occur in three East-Siberian Rivers, the Lena, Indigirka and Kolyma Rivers (van Dongen et al., 2008). A small set of sediments from a tropical river system (Tierney and Russell, 2009), showed an offset between the prevailing soil and river CBT/MBT values. Kim et al. (2012) compared the brGDGT distributions in the Amazon River SPM and sediments and soils from the Amazon watershed and concluded that aquatic

in situ production contributed to the riverine brGDGT pool. Zell et al. (2013) also described a different brGDGT distribution in soil and river brGDGTs in the Amazon River basin, characterized by a higher abundance of brGDGT Ia in soils. Furthermore, they investigated the intact polar lipid (IPL) precursors of brGDGTs. In living or recently living cells brGDGTs are present as IPLs which, after cell death, are relatively quickly degraded into core lipids (CL) (White et al., 1979) that are the compounds used in the CBT/MBT proxies. Both the presence of IPLs with a labile phosphatidyl headgroup and the similar distribution of the IPL-derived core lipids and the core lipids present in the SPM indicated riverine in situ production of brGDGTs.

In this study we examine for the first time the distribution of brGDGTs and crenarchaeol in the Yenisei River, the world's sixth largest river in terms of discharge that crosses Mongolia and Siberian Russia in a south to north direction. The large latitudinal range of the river (5500 km) allows us to evaluate changes in SPM brGDGT compositions that possibly derive from soil input from a watershed that crosses several climatic zones and vegetation types, i.e. the arid Mongolian steppe, the vast Russian boreal forest (Taiga and Tundra) and the Arctic. We sampled upstream tributaries and the main stream before and after major tributaries enter. The CBT/MBT′-derived pH and temperatures of the SPM are compared with soil pH and with the climate gradients present on the Eurasian continent. The amounts and distribution of IPL-derived CL are also evaluated. In addition, the environmental abundance of recently described hexamethylated isomers was assessed for the first time.

2. STUDY AREA

The Yenisei is the largest river in Russia and one of the largest rivers in Asia (Fig. 2A). The topographical properties are described in Degens et al. (1991). The river starts in Northern Mongolia and flows through the Central Siberian Plateau into the Kara Sea and the Arctic Ocean. Two large man-made lakes, the Krasnoyarsk reservoir and Sayano–Shushenskaya reservoir are situated in the upper reaches of the Yenisei. The river here has a high flow speed, a small riverbed width and little sedimentation. Further north, its most important tributary (25% of flow), the Angara River, joins the Yenisei. Angara River drains Lake Baikal, a large freshwater lake that is fed dominantly (50% of flow) by the Selenga River that drains large parts of Mongolia. The second important tributary for the Yenisei River is the Lower Tunguska (20% of flow). In the lower reaches of the river the Yenisei River flow becomes smooth, the riverbed width reaching several kilometers.

The mean annual discharge is estimated at 19,800 m^3/s. In this respect, the Yenisei takes ninth place among rivers worldwide (Telang et al., 1991). Dissolved organic carbon (DOC) is by far the dominant (>90%) form of organic carbon transported to the Arctic Ocean by the Yenisei (Lobbes et al., 2000). The Yenisei River is characterized by a pronounced discharge peak in June and relatively low water flow between September and April, with more than 30% of the annual discharge occurring in June (Stedmon et al., 2011; Fig. 2B). The annual discharge consists of 50% snowmelt, 35% rain water and approximately 15% groundwater (Pavlov and Pfirman, 1995).

The Yenisei River water catchment area equals 2.6×10^6 km^2. It extends for 5500 km in a south–north direction, covering different climate zones and biomes. Climate data, based on 13 Russian and 4 Mongolian weather stations that report daily temperature data, are summarized in Table 1. The climate is continental, with large seasonal temperature differences and a low mean annual temperature (MAT) over most of the territory. In the southernmost area, the MAT goes down to −6 °C, because of the high altitude. This increases slightly as the altitude effect decreases (Krasnoyarsk, MAT = 0.9 °C). Further north, the MAT decreases steadily, with a MAT of −11.4 °C in the most northern areas. Summer temperatures (June–September) decrease steadily from 15.4 °C in Mongolia to 2.9 °C in the north. Precipitation varies from >1000 mm yr^{-1} in the Sayan and Pytorana mountains and 300–600 mm yr^{-1} on the middle Siberian Plateau.

3. MATERIAL AND METHODS

3.1. Collection of SPM samples

Table 2 lists the river SPM samples investigated in this study and the sampling stations are shown in Fig. 2A. Surface water (<2 m depth) of the river (5–150 L) was collected and filtered (GF/F glass fiber filters, 0.7 μm pore size) at 12 locations distributed throughout Siberia. In August–September 2009, SPM from the Yenisei River water was collected with an in situ pump (McLane Large Volume Water Transfer System Sampler) employed from the R/V Sovetskaya Arktika, at 9 stations distributed along the Yenisei River. In 2010, three more SPM samples were obtained in tributaries of the Angara and in the Selenga River. Surface water was collected in canisters after wading several meters into the river and filtered using the same filters, a peristaltic pump and a titanium tripod system. Care was taken to sample flowing water in the river, avoiding zones with stagnant water. The water temperature ($n = 9$) and pH ($n = 3$) were measured immediately after collecting the water.

3.2. Lipid extraction and GDGT analyses

The freeze-dried filters were extracted using a modified Bligh and Dyer method as described by Pitcher et al. (2009). The filters were ultrasonically extracted three times for 10 min using a single-phase solvent mixture of MeOH/DCM/phosphate buffer 10:5:4 (v/v/v). The extract was separated into a core lipid (CL) and intact polar lipid (IPL) fraction over a small silica column, using a procedure modified from Pitcher et al. (2009), using hexane/ethyl acetate 1:1, v/v as eluent. An aliquot of the IPL fraction was analyzed directly for CL to check for potential carry-over into the IPL fraction. In order to analyze the IPL as CL, the extract was refluxed for a minimum of 2 h in 1.5 N HCl in MeOH. The amount of CL in this IPL-derived fraction was corrected for the amount of CL brGDGTs carried-

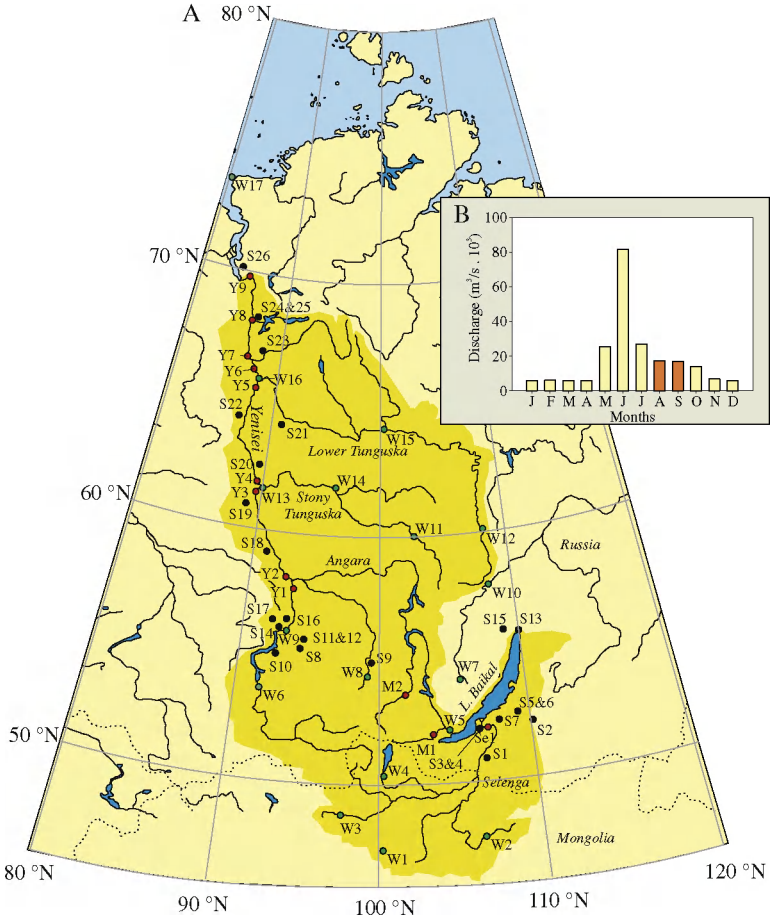

Fig. 2. (A) The Yenisei River and its catchment (indicated in dark yellow), located in Russian Siberia and Mongolia. Sampling stations (Table 2; Se1, M1–M2, Y1–Y9) are indicated with red dots, weather stations (Table 1; W1–W17) are indicated with green dots, soils included in the pH database (Table 3; S1–S26) are indicated with black dots. (B) Discharge regime of the Yenisei River. Months of sampling are indicated in orange.

Table 1
Weather stations; weather station code, coordinates and elevation. Climate data from the period 1963–2012 from the online NOAA database; Mean Annual Temperature (MAT), Mean Summer Temperature (MST), averaged from June to September.

Weather station		Latitude (°N)	Longitude (°E)	Elevation (m)	MAT (°C)	MST (°C)
W1	Bayanhongor	46° 07′48″	100° 40′ 48″	1859	0.0	15.4
W2	Ulaanbatar	47° 55′ 12″	106° 52′ 12″	1306	−1.6	15.4
W3	Tosontsengel	48° 43′ 48″	98° 12′ 00″	1723	−6.1	12.7
W4	Hatgal	50° 25′ 48″	100° 09′ 00″	1668	−4.6	10.6
W5	Irkutsk	52° 16′ 12″	104° 21′ 00″	498	−0.2	14.3
W6	Minusinsk	53° 43′ 12″	91° 42′ 00″	254	0.9	16.1
W7	Zhigalovo	54° 48′ 00″	105° 10′ 12″	418	−5.7	12.7
W8	Nizhneudinsk	54° 52′ 48″	99° 01′ 48″	411	0.7	13.9
W9	Krasnojarsk	56° 01′ 48″	92° 45′ 00″	276	0.9	14.8
W10	Kirensk	57° 46′ 12″	108° 04′ 12″	259	−3.9	13.9
W11	Vanavara	60° 19′ 48″	102° 16′ 12″	260	−5.7	12.7
W12	Erbogacen	61° 16′ 12″	108° 01′ 12″	291	−6.7	12.6
W13	Bor	61° 36′ 00″	90° 01′ 12″	58	−3.6	13.2
W14	Bajkit	61° 40′ 12″	96° 22′ 12″	262	−6.4	12.0
W15	Tura	64° 16′ 12″	100° 13′ 48″	168	−9.0	11.7
W16	Turuhansk	65° 46′ 48″	87° 55′ 48″	38	−6.4	11.4
W17	Dikson	73° 30′ 00″	80° 24′ 00″	47	−11.4	2.9

Table 2
Overview of the SPM sample stations in the Yenisei River catchment and their characteristics; sample codes, coordinates and sampling dates. The measured pH, surface water temperature and the particulate (>0.7 μm) organic carbon (POC) concentration per L are also given. N.d. indicates not determined values.

Station		Latitude (°N)	Longitude (°E)	Date sampled	Water T (°C)	Water pH	POC (mg. L^{-1})
Se1	Selenga River	51°43′41.8″	107°27′46.4″	06-07-2010	N.d.	8.4	649
M1	Irkut River	51°56′43.2″	100°47′18.2″	11-07-2010	10.8	5.6	12.0
M2	Uda River	54°51′22.7″	99°07′13.7″	30-06-2010	16.9	7.7	166
Y1	Yenisei River–Strelka	58°00′21.4″	93°55′48.3″	25-08-2009	12.0	N.d.	2.53
Y2	Yenisei River–Lesosibirsk	58°04′43.9″	92°55′28.2″	29-09-2009	11.0	N.d.	9.09
Y3	Yenisei River–Monastirsky Island	61°16′33.6″	90°54′0.18″	27-08-2009	N.d.	N.d.	17.1
Y4	Yenisei River–Stony Tunguska	61°28′30.4″	89°19′46.4″	25-09-2009	10.0	N.d.	3.33
Y5	Yenisei River–Kostino	65°11′32.4″	87°34′20.0″	29-08-2009	N.d.	N.d.	12.0
Y6	Yenisei River–Lower Tunguska	66°06′11.1″	87°08′24.0″	20-09-2009	9.0	N.d.	39.6
Y7	Yenisei River–Ledianaya Mt	66°21′19.1″	86°20′48.3″	31-08-2009	11.2	N.d.	17.7
Y8	Yenisei River–60 km south of Dudinka	68°24′27.6″	86°09′36.9″	01-09-2009	11.2	N.d.	6.95
Y9	Yenisei River–Seljanka Cape	69°25′22.9″	84°07′30.5″	03-09-2009	N.d.	N.d.	10.8

over. All GDGTs were quantified against a known amount of C_{46} GDGT standard (Huguet et al., 2006) that was added to each fraction before filtration through a 0.45 μm PTFE filter.

Samples were analyzed using a high performance liquid chromatography–mass spectrometry (HPLC–MS) method (Schouten et al., 2007). GDGTs were analyzed using an Agilent 1100 series/1100 MSD series instrument, with auto-injection system and HP-Chemstation software (Agilent Technologies). Injection volume was 10 μL. The HPLC system was fitted with a Prevail Cyano column (150 × 2.1 mm; 3 μm; Grace Discovery Sciences, USA). Separation was achieved at 30 °C with a flow-rate of 0.2 mL/min and the following gradient profile; 5 min hexane/propanol (99:1) with a gradual increase to hexane:isopropanol (98:2) after 45 min. The column was cleaned (back-flushing) for 10 min with hexane:isopropanol (90:10). Detection was achieved in selected ion monitoring mode (SIM; Schouten et al., 2007) using *m/z* 744 for the internal standard, *m/z* 1292 for crenarchaeol and *m/z* 1050, 1048, 1046, 1036, 1034, 1032, 1022, 1020 and 1018 for branched GDGTs. Agilent Chemstation software was used to integrate peak areas in the mass chromatograms of the protonated molecule ($[M+H]^+$) (Fig. 3B).

For an improved separation of the different isomers of the hexamethylated brGDGTs (De Jonge et al., 2013), a second HPLC–MS run was performed on an Agilent 1100 HPLC set-up, using a Prevail Silica column (150 × 2.1 mm; 3 μm; Grace Discovery Sciences, USA) at 30 °C with a flow rate of 0.2 mL/min. Elution was isocratically with hexane:isopropanol (97.8:2.2) for 38 min. The column was backflushed for 5 min with hexane:isopropanol (90:10). MS analysis was carried out on an Agilent 1100 MSD, in SIM mode, targeting *m/z* 1050, 1048, 1046, 1036, 1034, 1032, 1022, 1020 and 1018 for brGDGTs (Fig. 3C). The ratio between respectively IIIa and IIIa′, IIIb and IIIb′ and IIIc and IIIc′ was calculated based on the latter analysis. Subsequently, the obtained ratios were used to divide the the total amount of co-eluting brGDGTs, determined with the analysis performed on the cyano column according to Schouten et al. (2007).

Both datasets were integrated according to the NIOZ integration protocol (Schouten et al., 2009), where brGDGT isomers that are present as 'shoulders' are excluded from calculations. Careful evaluation of the chromatographic runs underlying the Weijers et al. (2007) and Peterse et al. (2012) calibrations showed that for soils the resolution on the cyano columns was not sufficient to identify, and thus quantify separately, brGDGT IIIa′, although analysis on a silica column revealed the presence of often abundant brGDGT hexamethylated isomers (Fig. 4). Therefore, the soil-derived MBT/MBT′ ratio actually used the combined relative abundance of brGDGT IIIa and IIIa′. In contrast, analysis of SPM from a Siberian lake and the Selenga river showed that the second isomer in aquatic environments can be partly separated on a cyano column (Fig 4). Therefore, the aquatic brGDGT calibrations (e.g. Pearson et al., 2011) are typically calculated using only IIIa but not IIIa′. The reason for this difference in chromatographic behavior is currently unknown, but is perhaps due to the difference in matrix between soil and aquatic samples.

3.3. Calculation of GDGT-based ratios and proxies

The relative amounts of the novel hexamethylated isomers are expressed as the isomer ratio (IR):

$$IR_{IIIx'} = IIIx'/(IIIx + IIIx'), \quad \text{where } x = \text{a, b, or c.}$$

The BIT index was calculated according to Hopmans et al. (2004):

$$\text{BIT index} = (Ia + IIa + IIIa)/(Ia + IIa + IIIa + IV).$$

The roman numerals refer to the GDGTs indicated in Fig. 1. Ia, IIa, and IIIa are brGDGTs and IV is the isoprenoid GDGT (iGDGT) crenarchaeol (specific GDGT for Thaumarchaeota; Sinninghe Damsté et al., 2000). The CBT and MBT′ indices (Peterse et al., 2012) were calculated as follows:

$$CBT = -\log((Ib + IIb)/(Ia + IIa))$$

and

$$MBT' = (Ia + Ib + Ic)/(Ia + Ib + Ic + IIa + IIb + IIc + IIIa + IIIa').$$

The MBT′ was calculated using both brGDGT IIIa and IIIa′, as the area of the peak of brGDGT IIIa as integrated by Peterse et al. (2012) represents the combined peak area of brGDGT IIIa and IIIa′.

For the calculation of pH and mean annual temperature (MAT), the global soil calibration of Peterse et al., 2012 was used (RSME denotes residual standard mean error):

$$pH = 7.9 - 1.97 * CBT (RSME = 0.8)$$

and.

$$MAT(^\circ C) = 0.81 - 5.67 * CBT + 31.0 * MBT' (RSME = 5.7\,^\circ C)$$

The mean summer temperature (MST) was calculated using a lake calibration (Pearson et al., 2011):

$$MST(^\circ C) = 20.9 + 98.1 * [Ib] - 12 * [IIa] - 20.5 * [IIIa] \times (RSME = 2.4\,^\circ C)$$

The square brackets in this formula indicate that the value is relative to the sum of the brGDGTs (Ia + IIa + IIIa + Ib + IIb + IIIb + Ic + IIc + IIIc).

3.4. Environmental parameters and bulk geochemical analysis

Soil pH data (Table 3) were obtained from published results (Santruckova et al., 2003), and accessible databases (Stolbovoi and Sheremet, 2002). The pH measurements reported in the Russian soil database were performed in a 1:5 soil/water mix, which results in pH values 0.1–0.5 units higher than those obtained from 1:2.5 soil/water ratios (Stolbovoi and Sheremet, 2002). We corrected for this offset by subtracting 0.5 pH units from the values provided. The particulate organic carbon (POC) content of river SPM samples on the filter was measured using a Flash 2000 Organic Elemental Analyzer.

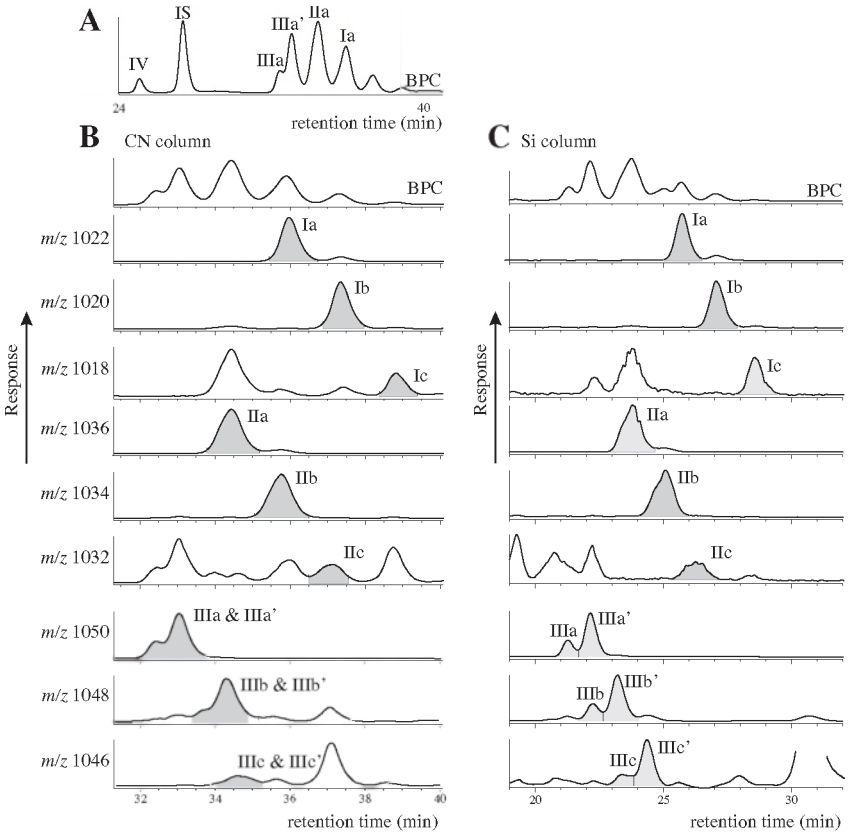

Fig. 3. (A) The base peak chromatogram of the SPM at station Se1; the compounds indicated are crenarchaeol (IV), internal standard (IS) and the brGDGTs Ia, IIa, IIIa and IIIa′ and (B) Base peak chromatogram and separate mass traces of the brGDGTs discussed in the text, after separation on a Prevail cyano (CN) column. (C) Base peak chromatogram and separate mass traces of the brGDGTs discussed in the text, after separation on a Prevail silica (Si) column. Note that the hexamethylated brGDGT isomers can be quantified using this method. Furthermore, the pentamethylated brGDGTs show a broader peak compared to the tetramethylated compounds, indicating the presence of a co-eluting compound.

3.5. Numerical analysis

The principal component analysis based on the correlation matrix was performed using the R software package for statistical computing. We performed an unconstrained Q-mode PCA on the standardized relative brGDGT values, excluding the relative amount of brGDGT IIIc and IIIc′, as the low abundance of these compounds did not allow quantification in several samples. The brGDGT scores are calculated proportional to the eigenvalues, and the site scores are calculated as the weighted sums of the species scores. The linear correlation coefficient between the $IR_{IIIa'}$ and $IR_{IIIb'}$ was calculated and the regression line plotted using the R software package for statistical computing.

4. RESULTS

4.1. Measured water parameters

Table 2 shows that the Yenisei River water temperature varied between 9.0 and 12 °C, with similar values for the mountainous Irkut River (10.8 °C) and higher values for the southern Selenga River (16.9 °C). The pH was measured only in three Yenisei tributaries and varied between 5.6 and 8.4.

4.2. Abundance of crenarchaeol and brGDGTs

In the CL fraction of Yenisei River SPM the concentration of crenarchaeol (0.0–3.1 ng L^{-1} and 0.0–6.6 ng g^{-1} POC) was an order of magnitude lower than that of the brGDGTs (0.3–69 ng L^{-1} and 29–470 ng g^{-1} POC) (Table 4). The dominance of brGDGTs in the SPM was reflected in high BIT index values, between 0.92 and 1.00 (Table 5). Crenarchaeol IPL percentages fluctuated between 21% and 45% in the river SPM. The IPL percentage of brGDGTs was generally lower, ranging from 5% to 20% (Table 4). The BIT value of the IPL fraction was up to 0.44 units lower than the BIT values of the CL fraction (Table 5).

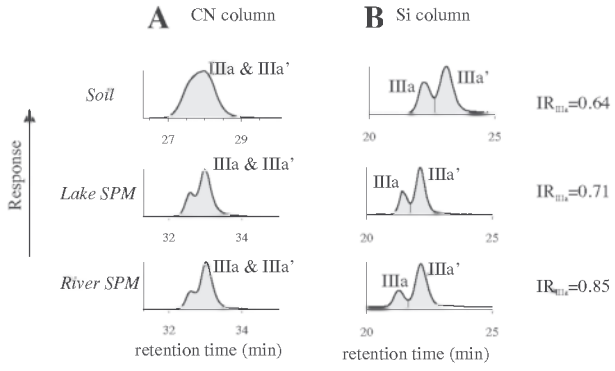

Fig. 4. The SIM chromatograms of the *m/z* 1050 of a soil (USA-CA2 from Peterse et al., 2012), lake SPM (Siberian "IL-Chir" lake, 51°N 96.166, 100°E 95.583) and river SPM (Se1); (A) contrasting the elution characteristics on a cyano column (Weijers et al., 2006a,b and Peterse et al., 2012) and (B) showing the similar $IR_{IIIa'}$ after elution on a silica column.

4.3. Distribution of brGDGTs

The relative abundances of individual brGDGTs in the CL and IPL fractions are given in Table 6. Fig. 3A illustrates a typical distribution of brGDGTs in the Yenisei SPM. BrGDGT CL distributions were dominated by brGDGTs without cyclopentane moieties. In the CL fractions of the river SPM, the recently described hexamethylated brGDGT IIIa′ (De Jonge et al., 2013) was the most abundant brGDGT in 6 out of 13 river SPM samples and second or third in abundance in the others (Table 6). In the IPL fraction, the brGDGT IIIa′ was the most abundant in 9 out of 13 samples. In the remaining samples, brGDGT IIa was the most abundant brGDGT. Application of a silica column for the separation of GDGTs (De Jonge et al., 2013) resulted in an improved separation of the hexamethylated brGDGT isomers (Fig. 3C). It is important to note that the pentamethylated brGDGT (IIa) has been shown to consist of two co-eluting isomers in a Siberian soil (De Jonge et al., 2013). Although the resolution was not good enough for separate quantification on the silica column (Fig. 3C), we observed a broad peak compared to the tetramethylated brGDGT and some separation, indicating the presence of a mixture of the two pentamethylated brGDGT isomers (IIa and IIa′) in Yenisei SPM.

The GDGT ratios were calculated according to Peterse et al. (2012), taking into account that for this calibration study the hexamethylated brGDGTs were not separated (see Section 3). The MBT′ value of both the CL and IPL fraction varied between 0.09 and 0.16. CBT values of the river SPM varied between 0.48 and 0.88 for the CL fraction and between 0.47 and 0.89 for the IPL fraction (Table 5).

5. DISCUSSION

5.1. The brGDGT distribution in Yenisei River SPM

The presence of an abundant partially co-eluting peak with brGDGT IIIa has been reported in Siberian Pleistocene loess-paleosol sequences by Zech et al. (2012). A second peak was also observed in a Siberian peat, collected in a lake floodplain, where the hexamethylated brGDGTs were shown to consist of four structurally distinct isomers (De Jonge et al., 2013). The first eluting peak contains the compound brGDGT IIIa as described by Weijers et al. (2006a), with two 5,13,16-trimethyloctacosane moieties and an asymmetrical molecule containing a 13,16-dimethyl octacosane and a 5,13,16,24-tetramethyl octacosane moiety. The second eluting peak (brGDGT IIIa′) contains two hexamethylated compounds, a brGDGT that possesses two 6,13,16-trimethyloctacosane moieties and an asymmetrical isomer containing a 13,16-dimethyl octacosane and a 6,13,16,23-tetramethyl octacosane moiety (De Jonge et al., 2013).

An improved chromatographic separation allowed us to quantify the brGDGTs IIIa′ in an environmental sampleset for the first time. The relative abundance of brGDGT IIIa′ in the SPM of the Yenisei is 22–51% of total of brGDGTs. Furthermore, the hexamethylated brGDGTs containing one and two cyclopentane moieties were also revealed as

Table 3
Descriptions and locations of soils samples used for describing the pH of the watershed soils.

	Soil type	Latitude (°N)	Longitude (°E)	Soil:water ratio	pH	Source [b]
S1	Cropland	51° 24′	107° 00′	1:5	6.4[a]	1
S2	Bog	52° 00′	110° 00′	1:5	6.5[a]	1
S3	Cropland	52° 00′	106° 25′	1:5	6.1[a]	1
S4	Forest	52° 00′	106° 24′	1:5	5.7[a]	1
S5	Cropland	55° 18′	109° 00′	1:5	6.3[a]	1
S6	Forest	55° 18′	109° 00′	1:5	6.7[a]	1
S7	Forest	55° 18′	108° 00′	1:5	4.5[a]	1
S8	Cropland	55° 00′	95° 00′	1:5	6.7[a]	1
S9	Forest	55° 00′	99°24′	1:5	4.2[a]	1
S10	Meadow	55° 11′	92° 18′	1:5	6.2[a]	1
S11	Cropland	55° 18′	95° 00′	1:5	6.8[a]	1
S12	Meadow	55° 18′	95° 00′	1:5	6.8[a]	1
S13	Bog	55° 29′	109° 32′	1:5	3.0[a]	1
S14	Meadow	56° 00′	92° 18′	1:5	6.4[a]	1
S15	Forest	56° 40′	108° 00′	1:5	6.4[a]	1
S16	Pine Forest	56° 24′	93° 00′	1:2	5.1	2
S17	Forest	56° 27′	91° 18′	1:5	4.6[a]	1
S18	Pine Forest	59° 24′	90° 00′	1:2	4.2	2
S19	Pine Forest	60 ° 30′	89° 00′	1:2	4.1	2
S20	Mixed Taiga	62° 30′	89° 00′	1:2	4.3	2
S21	Forest	64° 00′	92° 00′	1:5	5.7[a]	1
S22	Mixed Taiga	64° 18′	87° 30′	1:2	4.0	2
S23	Forest	67° 00′	90° 00′	1:5	4.0[a]	1
S24	Mixed Taiga	68° 05′	86° 42′	1:2	3.6	2
S25	Tundra	68° 05′	86° 42′	1:2	3.1	2
S26	Forest	70° 00′	84° 00′	1:5	4.8[a]	1

[a] Depending on the soil:water ratio used, the pH has been corrected with −0.5 units.
[b] Source of pH data: 1 = soils from the online database composed by Stolbovoi and McCallum (2002) and 2 = the soils described in Santruckova et al. (2003).

two peaks (Fig. 3B). These isomers are found in varying amounts (0.5–2.7% and 0.0–0.4% of total brGDGTs). A cross-plot of the $IR_{IIIa'}$ vs. $IR_{IIIb'}$ reveals a significant correlation (Fig. 5; p-value < 0.05). Although the $IR_{IIIc'}$ values plot closely to the $IR_{IIIb'}$ values, the dataset is too small to observe a significant correlation with $IR_{IIIa'}$. Because of this and the similar elution characteristics, we postulate that the hexamethylated brGDGTs with cyclopentyl moieties (IIIb and IIIc) also have later eluting isomers (IIIb′ and IIIc′) that are characterized by methyl groups at the α6 and ω6 position of the alkyl chains and are probably derived from the same biological source as IIIa′.

To investigate the general relationships between the branched GDGTs after quantification of all hexamethylated isomers using our improved chromatographic separation, we performed a principal component analysis (PCA) on the standardized relative abundances of the river SPM brGDGTs. The relative amounts of brGDGTs IIIc and IIIc′ have not been included, as they are present below the limit of quantification in the majority of the samples. The first three principal components represent 36%, 21% and 14% of the total variance, respectively (Fig. 6A and B). The scores provide us with a summary of the relationship between the stations and the variables (Fig. 6C and D).

The first principal component reflects the strong correlation between the relative abundance of the novel brGDGT isomers IIIa′ and IIIb′ (Fig. 6A) and illustrates their negative correlation with the relative abundance of brGDGT IIIa. SPM from the mountainous source area (M1 and M2) scores negatively on the first principal component (Fig. 6C), in line with the relatively low abundance of the novel brGDGT isomers IIIa′, IIIb′ and also brGDGT IIb (Fig. 6C) and high relative abundance of IIIa (Table 6). SPM collected from the main stream of the Yenisei River (Y2–Y7) scores higher on principal component 1 (Fig. 6C) and contains higher relative abundances of IIIa′ and IIIb′ (Table 6).

The pH and MAT were previously shown to explain most of the variation within the brGDGT distributions in soils globally (Weijers et al., 2007; Peterse et al., 2012). Also, earlier studies on the distribution of brGDGTs in freshwater environments have shown that mostly MAT/MST, but also pH to a varying degree, explain part of the variation in freshwater brGDGTs (Tierney et al., 2010; Pearson et al., 2011; Zhu et al., 2011). Our environmental dataset is incomplete and based on point-measurements, so it is impossible to assess to what extent the variation we observe is explained by pH and water temperature. However, the scores of the various brGDGTs on PC2 and PC3 seem to reflect their dependency on MAT and pH as described in the soil and lake calibrations studies. Weijers et al. (2007) and Peterse et al. (2010, 2012) have described an increase in cyclization of brGDGTs as a response to pH. This seems to be captured by the second principal component, where brGDGTs Ib, IIb and IIIb, all with one cyclopentane moiety, score high on the second

Table 4
The amounts of crenarchaeol and the total amount of brGDGTs expressed per L filtered (in ng L^{-1}) or expressed per amount of particulate OC (in ng g POC^{-1}). The amount of the IPL fraction is expressed relative to the total amount of CL and IPL (%). N.d. is not detected.

Station	Crenarchaeol (ng L^{-1})	Σ brGDGT (ng L^{-1})	Crenarchaeol (ng g POC^{-1})	Σ brGDGT (ng g POC^{-1})	Crenarchaeol IPL (%)	Σ brGDGT IPL (%)
Se1	3.1	69	4.7	110	41	5
M1	0.013	3.0	1.1	250	40	9
M2	0.057	4.8	0.34	29	45	12
Y1	0.017	0.63	6.6	250	26	10
Y2	0.025	4.3	2.7	470	34	10
Y3	0.060	5.3	3.5	310	21	9
Y4	N.d.	0.25	N.d.	75	N.d.	20
Y5	0.033	4.4	2.7	360	31	8
Y6	0.14	16	3.5	400	34	13
Y7	N.d.	4.3	N.d.	240	N.d.	11
Y8	0.014	1.7	1.9	240	23	7
Y9	0.041	1.7	1.3	160	22	6

principal component, as does the brGDGT Ic with two cyclopentane moieties. Especially the Selenga River SPM (Se1) scores high on this component, which is possibly related to differences in its watershed soil or water chemistry (Fig. 6D). The pH of the water sample at this station was indeed much higher than at other stations (Table 2), although there is only a single measurement. A high relative abundance of tetramethylated brGDGTs has been shown to be positively correlated to the MAT for a global soil dataset (Weijers et al., 2007; Peterse et al., 2012). This seems to be captured on the third principal component, where the tetramethylated brGDGTs Ia and Ic have a high positive loading while most hexamethylated brGDGTs and pentamethylated brGDGT IIc have negative loadings (Fig. 6C). Consistent with this hypothesis, the high mountainous station M1 plots separately on this component, indicating a cold signal (Fig. 6D). The IPL fractions typically score more negative than the corresponding CL fraction, consistent with the often lower relative abundance of brGDGT Ia and Ic in the IPL fraction (Table 5). We hypothesize that the offset in the living or recently living material is caused by the colder temperature in September compared to July/August for the Yenisei samples. The SPM collected at site Se1 may carry a warmer CL signal from the downstream Mongolian steppe.

5.2. Sources of brGDGTs in the Yenisei River

Analysis of the river SPM shows the presence of the full suite of brGDGTs in the river SPM, in both the core lipid (CL) and intact polar lipid (IPL) fractions. Their presence fits with the hypothesis that transport of brGDGTs by rivers is a mechanism for the delivery of these lipids to coastal marine sediments (Hopmans et al., 2004). The BIT indices of the CL fraction of the riverine SPM ranged from 0.94 to 0.99 (Table 5), at least as high as BIT-values encountered in global soils (Hopmans et al., 2004; Weijers et al., 2006b; Schouten et al., 2013). The BIT-index reported here is comparable to the values encountered in the Amazon River SPM (Kim et al., 2012; Zell et al., 2013) and Yangtze River sediments, China (Zhu et al., 2011; Yang et al., 2013) and higher than values reported for SPM from the Têt and Rhone River, France (Kim et al., 2007) and the Rhine and Meuse, N-Europe (Herfort et al., 2006). However, when comparing BIT values, it is important to keep in mind that absolute values may vary between labs (Schouten et al., 2009).

BrGDGTs in aquatic systems can be derived from two major sources. First, they are eroded from watershed soils and transported with run-off (Weijers et al., 2007). Secondly, brGDGTs are produced by micro-organisms living within fresh and marine water systems (Tierney and Russell, 2009; Peterse et al., 2009). The resulting distribution will thus often be a mixture of both sources, complicating the interpretation of MBT/CBT proxies. Previous studies on the brGDGT distributions have recognized systems that are dominated by soil input (Niemann et al., 2012), by in situ production (e.g. Tierney et al., 2012) or by a mixture of these end members (e.g. Zell et al., 2013). For the Yenisei River, distributions dominated by soil-input would be expected to reflect the low pH of the catchment soils (Table 3) and the strong temperature gradient imposed on the soils (Table 1). On the other hand, brGDGTs produced in situ in the river water should reflect its characteristics: the absence of a strong temperature gradient and a stable pH of ca. 7.

The PCA analysis revealed that variations in the brGDGT distributions may partly be explained by changes in pH and temperature as has been reported before for other environmental datasets. Therefore, it is a logical approach to calculate pH and temperature from the brGDGT composition to shed light on their origin. We have reconstructed variations in MAT and pH using both soil (Peterse et al., 2012) and lake calibrations (Pearson et al., 2011). A complication in this respect is the relatively high abundance of 6-methyl isomers of the hexamethylated brGDGTs in Yenisei SPM (Table 6), since the presence of these components was unknown at the time of these calibrations. Since all published studies on soil calibrations used LC separation methods that did not separate these isomers (see Section 3), we used the summed relative abundance of the 5- and 6-methyl isomers in these calculations. The lake calibration

Table 5
Overview of BIT, CBT, MBT, reconstructed pH, reconstructed MAT using the soil calibration (Peterse et al., 2012) and reconstructed MST using the lake calibration (Pearson et al., 2011).

Station	Lipid type	BIT	CBT	MBT′	Calc pH	Calculated MAT (°C) Soil calibration	Calculated MST (°C) Lake calibration
Se1	CL	0.92	0.48	0.16	7.0	2.9	19.6
	IPL	0.48	0.47	0.14	7.0	2.5	18.2
M1	CL	0.99	0.88	0.10	6.2	−1.2	10.5
	IPL	0.96	0.89	0.13	6.1	−0.2	11.3
M2	CL	0.98	0.85	0.14	6.2	0.5	12.1
	IPL	0.90	0.83	0.15	6.3	0.8	13.4
Y1	CL	0.95	0.67	0.14	6.6	1.5	16.6
	IPL	0.83	0.72	0.10	6.5	−0.1	16.0
Y2	CL	0.99	0.53	0.08	6.8	0.4	14.9
	IPL	0.93	0.54	0.09	6.8	0.6	16.2
Y3	CL	0.97	0.67	0.14	6.6	1.4	16.5
	IPL	0.93	0.61	0.11	6.7	0.8	15.8
Y4	CL	1.00	0.64	0.13	6.6	1.1	15.6
	IPL	1.00	0.57	0.15	6.8	2.2	16.9
Y5	CL	0.98	0.64	0.14	6.6	1.4	16.3
	IPL	0.92	0.57	0.12	6.8	1.4	15.9
Y6	CL	0.98	0.59	0.12	6.7	1.1	14.2
	IPL	0.93	0.54	0.13	6.8	1.9	17.1
Y7	CL	1.00	0.73	0.13	6.5	0.7	15.1
	IPL	1.00	0.72	0.10	6.5	−0.1	14.5
Y8	CL	0.99	0.75	0.16	6.4	1.5	14.6
	IPL	0.94	0.71	0.14	6.5	1.1	15.1
Y9	CL	0.99	0.78	0.16	6.4	1.3	14.2
	IPL	0.94	0.73	0.13	6.5	0.8	14.3

Table 6
Overview of the relative abundance of individual brGDGTs of the CL and IPL fractions. N.d. is not detected.

Station	Lipid type	Relative amount per compound (%)											
		Ia	Ib	Ic	IIa [a]	IIb [a]	IIc [a]	IIIa	IIIa′	IIIb	IIIb′	IIIc	IIIc′
Se1	CL	10.3	4.3	0.6	32.0	9.7	0.6	5.8	34.4	0.5	1.6	0.1	0.2
	IPL	9.2	3.9	0.5	30.8	9.5	1.6	9.3	32.4	0.9	1.7	N.d.	N.d.
M1	CL	7.8	1.7	0.2	30.0	3.3	2.8	28.1	25.3	0.4	0.5	N.d.	N.d.
	IPL	10.5	2.0	0.3	31.4	3.4	0.6	26.5	23.3	0.7	1.3	N.d.	N.d.
M2	CL	11.9	2.0	0.3	30.2	4.0	0.5	22.9	27.0	0.5	0.6	N.d.	N.d.
	IPL	12.3	2.2	0.4	29.5	4.0	1.8	19.1	29.7	0.3	0.7	N.d.	N.d.
Y1	CL	10.2	3.0	1.0	27.4	5.1	0.8	10.6	40.5	0.4	0.9	N.d.	N.d.
	IPL	9.0	2.1	N.d.	25.3	4.4	0.9	7.0	49.8	0.4	1.1	N.d.	N.d.
Y2	CL	6.1	1.8	0.2	32.0	9.4	0.3	6.4	41.0	0.4	2.1	0.0	0.3
	IPL	6.8	2.2	0.1	22.5	6.2	0.7	7.9	50.6	0.5	2.7	N.d.	N.d.
Y3	CL	11.3	2.0	0.4	27.1	6.1	0.4	5.3	44.6	0.2	2.1	0.1	0.3
	IPL	8.9	1.8	0.3	25.1	6.5	0.9	6.4	47.4	0.5	2.2	N.d.	N.d.
Y4	CL	9.6	2.0	0.8	24.6	5.8	0.5	8.7	45.6	0.4	2.1	N.d.	N.d.
	IPL	11.7	2.7	N.d.	24.4	6.9	1.1	10.2	39.9	1.0	2.1	N.d.	N.d.
Y5	CL	10.7	2.1	0.4	27.2	6.6	0.4	6.2	43.4	0.5	1.9	0.1	0.3
	IPL	9.1	2.4	0.5	26.0	7.1	1.4	10.0	41.0	0.8	1.8	N.d.	N.d.
Y6	CL	8.8	2.0	0.4	24.4	6.6	0.4	14.0	40.1	0.6	2.2	0.1	0.4
	IPL	10.0	2.5	0.4	24.1	7.3	0.9	8.0	43.5	0.5	2.7	N.d.	N.d.
Y7	CL	10.4	1.8	0.3	26.8	5.1	0.3	7.9	44.8	0.5	1.7	0.0	0.3
	IPL	8.2	1.5	0.2	25.2	4.8	0.4	7.8	49.1	0.6	2.2	N.d.	N.d.
Y8	CL	13.0	2.2	0.4	29.6	5.4	0.5	12.9	34.2	0.4	1.4	N.d.	N.d.
	IPL	10.9	2.6	0.1	28.6	5.0	0.7	13.2	36.6	0.4	1.8	N.d.	N.d.
Y9	CL	13.2	2.0	0.4	29.8	5.1	0.5	13.6	33.5	0.6	1.3	N.d.	N.d.
	IPL	10.6	2.4	0.1	28.7	5.0	0.5	15.2	35.2	0.8	1.6	N.d.	N.d.

[a] In a Siberian peat in the Yenisei watershed, IIa was shown to consist of two isomers that co-elute (De Jonge et al., 2013). In this study, the contribution of isomers to the areas of IIa, IIb and IIc is probable but remains to be proven.

is based on the abundance of brGDGT IIIa after exclusion of brGDGT IIIa′, according to commonly adopted integration protocols (Schouten et al., 2009). For the aquatic calibration, we thus use only the area of brGDGT IIIa but not of IIIa′.

Based on the chromatograms (Fig. 3), it is likely that, next to the presence of large amounts of hexamethylated brGDGT isomers, a substantial amount of 6-methyl isomers of the pentamethylated compounds (IIa, IIb and IIc) is present. The effect of the presence of these pentamethylated isomers on the proxy calculations is possibly large, as this isomer of brGDGT IIa was shown to equal 50% of the total amount of brGDGT IIa in a Siberian peat, collected in a lake floodplain (De Jonge et al., 2013).

5.3. The CBT-index and reconstructed river pH

Based on the global soil calibration by Peterse et al. (2012), the reconstructed pH varies between 6.1 and 6.9 for the CL fraction (Table 5). The pH is uniform downstream, with slightly lower values in SPM originating closer to the mountainous source area of the Yenisei and at high latitudes (Table 5, Fig. 7A). The IPL fraction-based pH (6.1–7.0) mimics that of the CL fraction closely, with a maximum offset of 0.15 pH units. Overall, the pH values are substantially higher than those of soils in the Yenisei watershed (pH 3.0–6.8, Table 3, Fig. 8).

Taking into account the pH reconstruction calibration error of 0.8 (Peterse et al., 2012), only soils with pH values >5.3 are likely sources of these brGDGTs. However, such soils are only encountered in the southern part of the watershed (between 52 and 56°N), in agriculturally more developed and forested areas (Table 3). The northern part of the watershed (an extensive area of low pH peatland that typically contains high amounts of brGDGTs (cf. Weijers et al., 2006a)) is expected to contribute brGDGTs with a low degree of cyclisation (resulting from the low pH), as it sources two major tributaries of the Yenisei River. However, a decrease of the reconstructed pH from brGDGTs in riverine SPM after the inflow of these tributaries is not evident and, therefore, it is unlikely that the brGDGTs in the riverine SPM are predominantly soil-derived. Consequently, we propose that the brGDGTs in the Yenisei River SPM are primarily derived from in situ production since the reconstructed pH is close to that of the river water. The similar reconstructed pH values of the IPL fraction supports this hypothesis, as this value is likely to reflect living or recently living biomass.

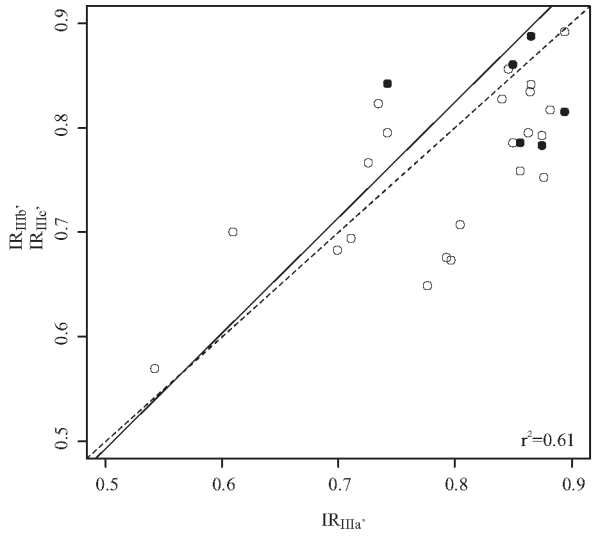

Fig. 5. A cross-plot comparing the isomer ratios (IR) of the brGDGT IIIa′ versus the IR of brGDGT IIIb′ (white symbols) and IIIc′ (black symbols). The linear regression line between $IR_{IIIa'}$ and $IR_{IIIb'}$ is plotted with a full line and the corresponding correlation coefficient (r^2) value given. The 1:1 ratio is plotted with a dotted line.

CBT-reconstructed pH values have been previously reported for riverbed sediments and match river water pH (Tierney and Russell, 2009; Tierney et al., 2010; Zhu et al., 2011; Yang et al., 2013). The pH of the Yenisei River is reported to be constant downstream and over time (Sorokovikova, 1997), with values between 7.0 and 7.3 (±0.2) along the river. The reconstructed pH values (between 6.1 and 6.8) are only slightly lower than the Yenisei River water pH. This offset is larger for the more alkaline upstream rivers. Here, the measured pH values are more variable and reconstructed pH values do not reflect the magnitude of these variations well (Table 5; Fig. 7A). This larger offset is most probably due to the variation in pH (up to 2 pH units daily) that has been encountered in weakly buffered alkaline streams (Nimick et al., 2011).

5.3.1. Reconstruction of temperatures

Similar to the pH values, MBT′/CBT-reconstructed temperatures using the soil calibration along the main part of the Yenisei River are remarkably constant (Fig. 7B). They do not reflect the large changes in MAT imposed on the soils from south to north (from 0.9 to −10 °C; Table 1). The reconstructed Yenisei SPM MAT varies between −1.2 and 2.9 °C, which is up to 9 °C higher than the observed MAT imposed on local and upstream soils (Fig. 7B). Thus, both the absolute values of MAT reconstructed and the absence of a north–south trend do not fit with the MAT imposed on the soils of the watershed. To test whether the distributions fit with a freshwater source, we use a global lake calibration that is based on the MST (Pearson et al., 2011). The reconstructed temperatures of the main stream are between 14.2 and 17.1 °C for both the IPL and CL fractions (Table 5; Fig. 7C), which is only slightly higher than the measured temperatures at the time of sampling (Table 2). The absolute values of this MST reconstruction fit the MST temperatures of weather stations in the area of the upper reaches of the Yenisei River (Fig. 7). The MST of weather stations at higher latitudes is somewhat lower than the reconstructed MST but this is in line with the fact that warmer river water is transported towards higher latitudes before it can adjust to the colder MST downstream. In situ production of brGDGTs in the river water can thus account for the absence of a latitudinal gradient in the brGDGT distributions. The temperatures reconstructed for the mountainous upstream rivers also give a reliable temperature estimate. The mountainous riv-

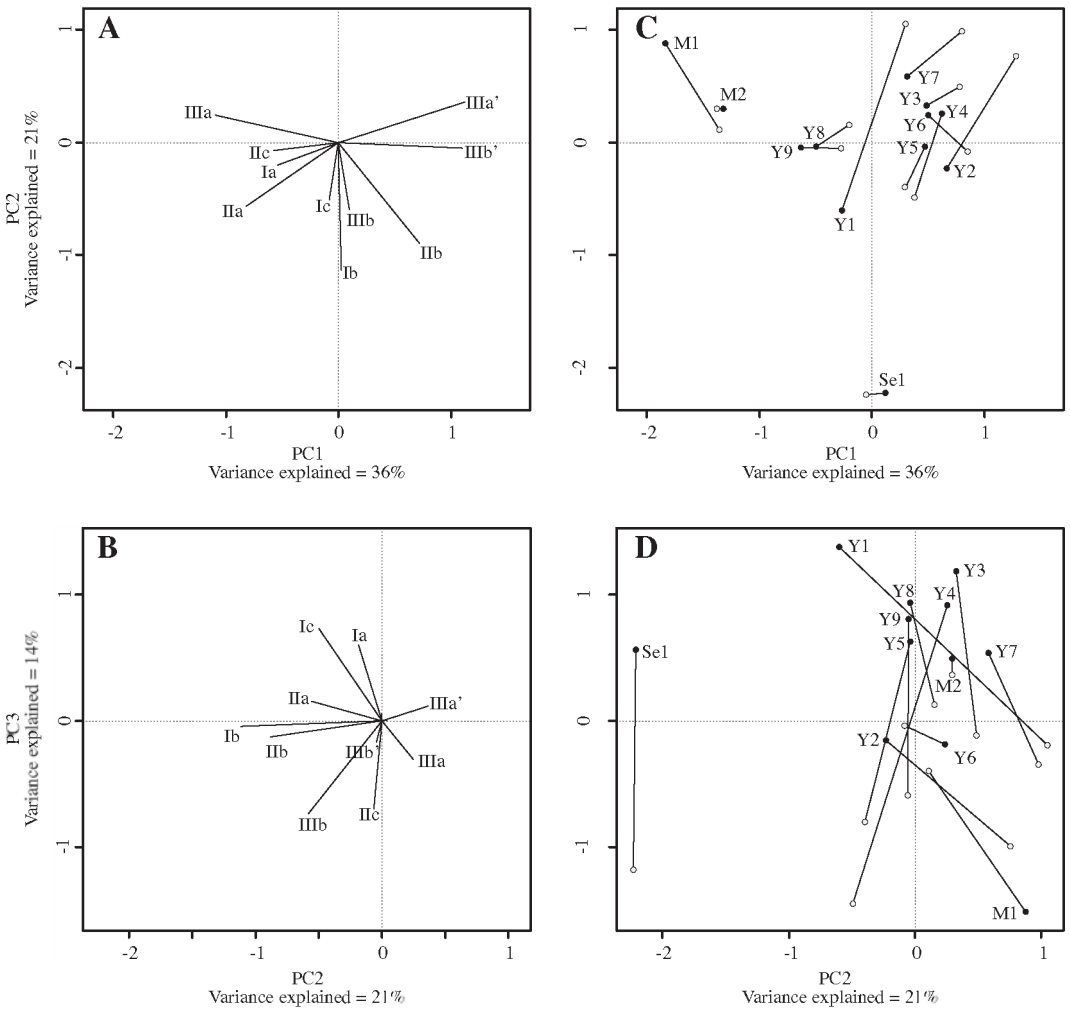

Fig. 6. Biplot of the principal component analysis based on the relative abundance of the river SPM brGDGTs. The loadings of the variables (A, B) and the scores of the sites (C, D) are plotted on the first three components. The first component accounts for 36% of the variance, the second component for 21%, the third component for 14%. The score of each station is calculated using the relative abundance of each compound per station and its loading on the PC. Scores based on a CL fraction are indicated with a black symbol and per station connected with the scores based on the IPL fraction, indicated with a grey symbol.

ers that flow into the Angara River and the SPM downstream the inflow of the Angara River shows a contribution of a colder signal (Table 5, Fig. 7B).

5.3.2. *Importance of in situ produced versus soil-derived brGDGTs*

Based on the distribution of brGDGTs, this study thus indicates that the Yenisei River is an example of a river system where brGDGTs are dominantly produced in situ. This is in contrast with previous studies by Kim et al. (2012) and Zell et al. (2013) on the Amazon River that concluded that soils are the dominant source of brGDGTs (70–80%). On the other hand, Zhu et al. (2011) concluded that the brGDGT signal of the Yangtze River catchment was overprinted by brGDGTs produced in situ. Based on a study in a hydroplant lake situated on the same river, Yang et al. (2013) endorsed this conclusion. The relative contribution of in situ produced brGDGTs is thus variable between river systems.

We postulate that the contribution of in situ produced brGDGTs is dominant in the Yenisei River because of the relatively low amounts of soil-derived brGDGTs. This is supported by the relatively low concentrations of brGDGTs present in the SPM (Table 4). The concentration of brGDGTs in the Selenga River is comparable to previous studies of rivers in France and Northern Europe (Herfort et al., 2006; Kim et al., 2007), but it is up to an order of magnitude lower than found in the Amazon River (Kim et al., 2012). The concentration of GDGTs at the other stations is lower, only comparable to the Têt and Rhone rivers during time periods other than flood events (Kim et al., 2007). The higher brGDGT concentration in the Selenga River corresponds with a high amount of POC. Normalized on the POC content, the brGDGT concentrations are similar at all stations (Table 4). In this way, brGDGT concentrations at all stations are comparable to the lowest values reported from the European Rivers (Herfort et al., 2006; Kim et al., 2007), but two orders of magnitude lower than

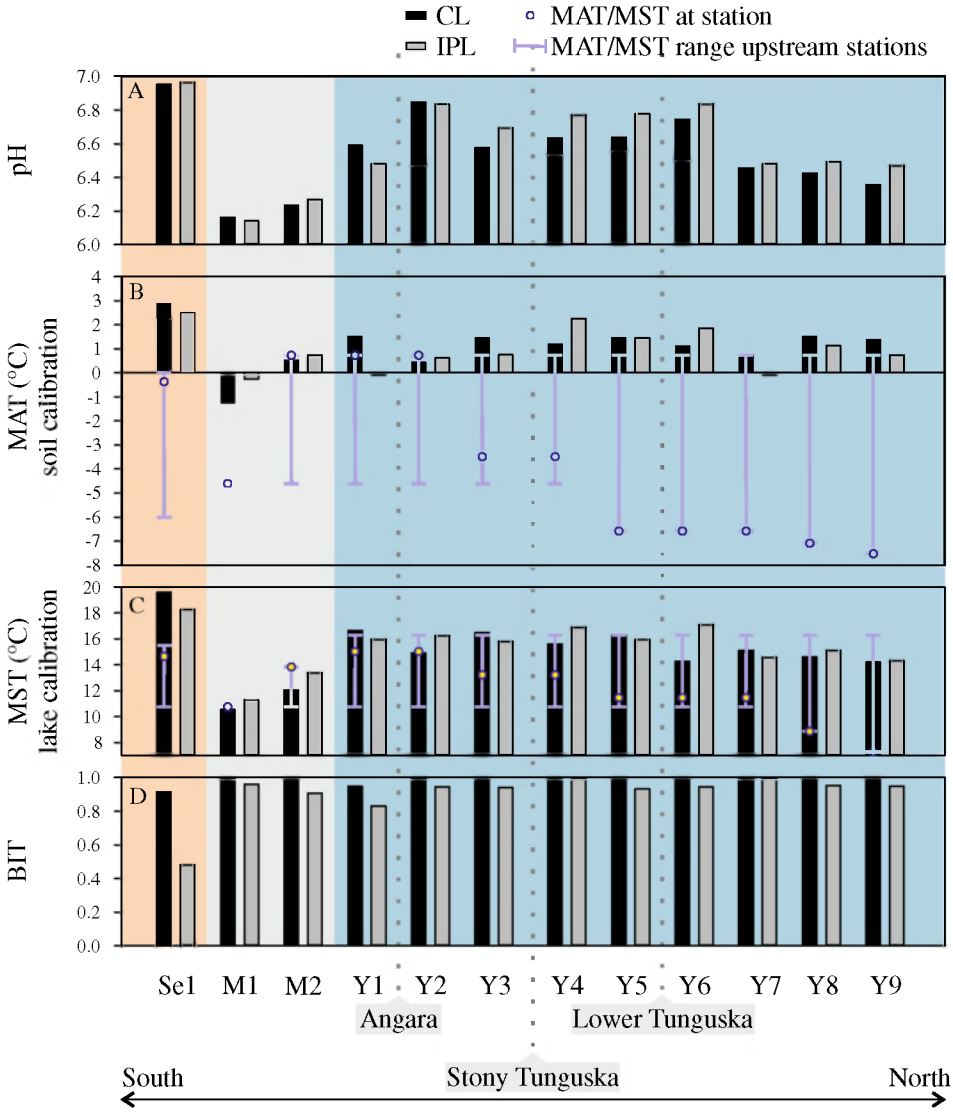

Fig. 7. Barplots showing the variation in GDGT-based proxies, from south to north. Black bars are values based on the CL fraction, grey bars are the values based on the IPL fraction. Background colors denote tributaries from different parts of the watershed. Orange; Selenga watershed. Grey; Angara watershed. Blue; Yenisei River samples. The dotted grey line shows where major tributaries drain in the Yenisei River. (A) Reconstructed pH. (B) reconstructed MAT, based on the soil calibration, represented by the black and grey bars. The MAT of all upstream weather stations is summarized by the purple line. The yellow dot indicates the MAT at the station. (C) Reconstructed MST, based on the lake calibration, represented by the black and grey bars. The MST of all upstream weather stations is summarized in the purple line. The yellow dot indicates the MST at the station. (D) BIT-index.

the values reported for the Amazon River during the low water season (Kim et al., 2012; Zell et al., 2013) and up to three orders of magnitude lower than the values reported for the high water season (Kim et al., 2012).

The niche of the aquatic brGDGT source organisms can be twofold; first, it can be derived from the water-logged wetlands around shallow lakes that source the Yenisei River water. Water-logged soils have been described to have a brGDGT distribution more alike lakes (Loomis et al., 2011). We studied brGDGTs in one peat, obtained from the floodplain of a lake (De Jonge et al., 2013). Its brGDGT distributions was indeed similar to that of the river SPM at site M1, sampled slightly downstream (pH reconstructed = 6.7, MAT reconstructed = 0.7), suggesting a shared source. Or, the brGDGTs can be produced in the river channel itself, if time allows the build-up of detectable concentrations of brGDGTs. The residence time of the SPM can be estimated based on the propagation speed and the length of the river. Using the propagation speed of the Lena River, a major Siberian River located east of the Yenisei, of 88 km day^{-1} (Smith and Pavelsky, 2008), we can calculate a water transport time of 62 days, from source to the river mouth. This is a minimum for the residence time of the SPM, as all natural river channels contain "dead zones", or areas of low velocity. Mixing processes carry suspended sediment into these low-velocity zones where particles settle out and accumulate until they are resuspended and transported further downstream. Thus,

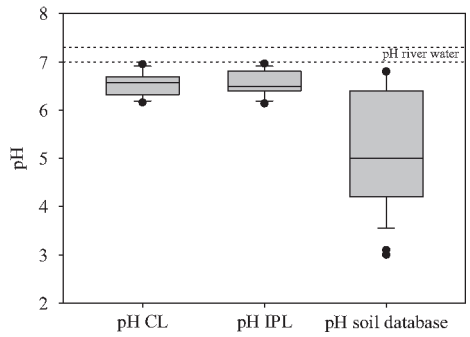

Fig. 8. Comparison of boxplots of the reconstructed pH based on the CL fraction and IPL fraction with the pH values from the soil database and the Yenisei River water. The first, second and third quartiles are indicated.

these zones can act as a source area for the bacterial population. Furthermore, bacterial cells and lipids can be sourced from the hyporheic zone, the layer of saturated sediments and surface water beneath the river channel (Dobson, 1998). During the summer season, turnover times for attached and free-living bacteria in rivers have been reported by Edwards and Meyer (1986), to be in the order of 2 weeks. This is significantly shorter than the residence time, aquatic production in the river water itself thus seems plausible. The time required for the IPL fraction to be (partly) degraded to CL strongly depends on the polar headgroup. BrGDGT lipids with a labile phosphatidyl headgroup have been described in the Amazon River SPM by Zell et al. (2013), where they indicate freshly produced material.

The low amount of soil-derived brGDGTs in the Yenisei River can be explained by a low amount of horizontal runoff during the sampling season. The SPM samples were taken several months after the freshet, when the precipitation that accumulated as a snow layer during autumn, winter and spring is released as a large meltwater pulse into the Kara Sea. About 30% of the total annual water budget and 42% of the total annual sediment budget are discharged in June (Lammers and Shiklomanov, 2000). This indicates that the brGDGT signal in the Yenisei River SPM may thus be very different during the freshet, and an integrated annual signal may possibly match the soil brGDGT signature better.

6. CONCLUSIONS

This study represents the first comprehensive record of brGDGT distribution in a river that crosses several climatic zones in a north–south direction, revealing insights in the site of their production. At all stations, in both the CL and IPL fraction, the full suite of brGDGTs is present. The brGDGT distribution is uniform downstream, in contrast to the strong climate gradients crossed. As the reconstructed pH is too high for the surrounding soils and the gradient in MAT of the Yenisei watershed is not reconstructed, we conclude that brGDGTs in the SPM of the Yenisei River and tributaries do not reflect the watershed soil characteristics. The absence of strong changes in the distribution can be explained if the brGDGTs are produced in the river water, as it has a relatively constant pH and temperature downstream. The pH of the river water is reconstructed well using the soil calibration and the MST is reconstructed well using a lake calibration. The brGDGTs in the Yenisei River and tributary SPM thus likely reflect an in situ produced aquatic signal. The absence of a soil-derived signal can be due to the low soil input at the time of sampling (end of summer). We hypothesize that the SPM signal of the Yenisei River may be highly seasonal, as much more soil material will be transported in the river during the freshet. To assess these seasonal changes, further research is required.

The exceptional brGDGT distribution of the Yenisei SPM was shown to be dominated by the newly described brGDGT IIIa′. This compound was shown to be an important constituent of the brGDGTs in the SPM (between 22% and 51% of all brGDGTs). The chromatographically similar isomers brGDGTs IIIb′ and IIIc′ are tentatively identified as having the same shift in methylation from the α5 and/or ω5 to the α6 and/or ω6 position. Also, the chromatography of the pentamethylated brGDGT IIa and IIb in the dataset suggests the presence of an isomer with methylation at the α6 and/or ω6 position.

At the moment it is unclear if both isomeric forms are biosynthesized independently, or if isomers with a methylation on the α6 position are produced as an alternative to the corresponding isomer with a methylation on the α5 position of the alkyl chain. If they are biosynthesized independently, it is unknown if these compounds react independently to environmental factors. The hexamethylated brGDGT isomers have been included in soil calibration as defined in Weijers et al. (2007) and Peterse et al. (2012) and excluded from lake calibrations (Pearson et al., 2011), following integration protocols. Using an improved chromatographic method, this study and previous studies indicate that these isomers can be abundant in the environment. Improving the separation and quantifying the hexa- and pentamethylated isomers will be required to assess the relevance of these isomers for the pH and temperature reconstruction. The logical next step will be to recalibrate the soil and lake calibrations and to evaluate if the exclusion or inclusion of hexa- and pentamethylated brGDGT isomers can explain some of the scatter observed in these calibrations.

ACKNOWLEDGMENTS

The three anonymous reviewers are thanked for providing constructive comments that have improved this manuscript. This work, performed in the framework of the memorandum NIOZ-VNIIOkeangeologia for Arctic research, was funded by research project 819.01.013, financed by the Netherlands Organization for Scientific Research (NWO) and the European Research Council under the EU Seventh Framework Programme (FP7/2007-2013)/ERC grant agreement No. [226600].

REFERENCES

Bendle J. A., Weijers J. W. H., Maslin M. A., Sinninghe Damsté J. S., Schouten S., Hopmans E. C., Boot C. S. and Pancost R. D.

(2010) Major changes in glacial and Holocene terrestrial temperatures and sources of organic carbon recorded in the Amazon fan by tetraether lipids. *Geochem. Geophys. Geosyst.* **11**.

Blaga C. I., Reichart G. J., Heiri O. and Sinninghe Damsté J. S. (2009) Tetraether membrane lipid distributions in water-column particulate matter and sediments: a study of 47 European lakes along a north–south transect. *J. Paleolimnol.* **41**, 523–540.

Blaga C. I., Reichart G. J., Schouten S., Lotter A. F., Werne J. P., Kosten S., Mazzeo N., Lacerot G. and Sinninghe Damsté J. S. (2010) Branched glycerol dialkyl glycerol tetraethers in lake sediments: can they be used as temperature and pH proxies? *Org. Geochem.* **41**, 1225–1234.

De Jonge C., Hopmans E. C., Stadnitskaia A., Rijpstra W. I. C., Hofland R., Tegelaar E. and Sinninghe Damsté J. S. (2013) Identification of novel penta- and hexamethylated branched glycerol dialkyl glycerol tetraethers in peat using HPLC–MS^2, GC–MS and GC–SMB-MS. *Org. Geochem.* **54**, 78–82.

Degens E.T., Kempe S., Richey J.E. (1991) Biogeochemistry of major world rivers. Published on behalf of the Scientific Committee on Problems of the Environment (SCOPE) of the International Council of Scientific Unions (ICSU), and the United Nations Environment Programme (UNEP) by Wiley, Chichester; New York.

Dobson M. (1998) *Ecology of Aquatic Systems*. Longman, Harlow, Essex, England.

Donders T. H., Weijers J. W. H., Munsterman D. K., Hoeve M. L. K., Buckles L. K., Pancost R. D., Schouten S., Sinninghe Damsté J. S. and Brinkhuis H. (2009) Strong climate coupling of terrestrial and marine environments in the Miocene of northwest Europe. *Earth Planet. Sci. Lett.* **281**, 215–225.

Edwards R. T. and Meyer J. L. (1986) Production and Turnover of Planktonic Bacteria in two Southeastern Blackwater Rivers. *Appl. Environ. Microbiol.* **52**, 1317–1323.

Herfort L., Schouten S., Boon J. P., Woltering M., Baas M., Weiers J. W. H. and Sinninghe Damsté J. S. (2006) Characterization of transport and deposition of terrestrial organic matter in the southern North Sea using the BIT index. *Limnol. Oceanogr.* **51**, 2196–2205.

Hopmans E. C., Weijers J. W. H., Schefuß E., Herfort L., Sinninghe Damsté J. S. and Schouten S. (2004) A novel proxy for terrestrial organic matter in sediments based on branched and isoprenoid tetraether lipids. *Earth Planet. Sci. Lett.* **224**, 107–116.

Huguet C., Hopmans E. C., Febo-Ayala W., Thompson D. H., Sinninghe Damsté J. S. and Schouten S. (2006) An improved method to determine the absolute abundance of glycerol dibiphytanyl glycerol tetraether lipids. *Org. Geochem.* **37**, 1036–1041.

Kim J.-H., Ludwig W., Schouten S., Kerherve P., Herfort L., Bonnin J. and Sinninghe Damsté J. S. (2007) Impact of flood events on the transport of terrestrial organic matter to the ocean: a study of the Tet River (SW France) using the BIT index. *Org. Geochem.* **38**, 1593–1606.

Kim J.-H., Zell C., Moreira-Turcq P., Perez M. A. P., Abril G., Mortillaro J.-M., Weijers J. W. H., Meziane T. and Sinninghe Damsté J. S. (2012) Tracing soil organic carbon in the lower Amazon River and its tributaries using GDGT distributions and bulk organic matter properties. *Geochim. Cosmochim. Acta* **90**, 163–180.

Lammers R.B. and Shiklomanov A.I. (2000) R-ArcticNet, A Regional Hydrographic Data Network for the Pan-Arctic Region, Durham, NH: Water Systems Analysis Group, University of New Hampshire; distributed by the National Snow and Ice Data Center.

Lobbes J. M., Fitznar H. P. and Kattner G. (2000) Biogeochemical characteristics of dissolved and particulate organic matter in Russian rivers entering the Arctic Ocean. *Geochim. Cosmochim. Acta* **64**, 2973–2983.

Loomis S. E., Russell J. M. and Sinninghe Damsté J. S. (2011) Distributions of branched GDGTs in soils and lake sediments from western Uganda: implications for a lacustrine paleothermometer. *Org. Geochem.* **42**, 739–751.

Loomis S. E., Russell J. M., Ladd B., Street-Perrott F. A. and Sinninghe Damsté J. S. (2012) Calibration and application of the branched GDGT temperature proxy on East African lake sediments. *Earth Planet. Sci. Lett.*, 357–358, 277–288.

Niemann H., Stadnitskaia A., Wirth S. B., Gilli A., Anselmetti F. S., Sinninghe Damsté J. S., Schouten S., Hopmans E. C. and Lehmann M. F. (2012) Bacterial GDGTs in Holocene sediments and catchment soils of a high Alpine lake: application of the MBT/CBT-paleothermometer. *Climate Past* **8**, 889–906.

Nimick D. A., Gammons C. H. and Parker S. R. (2011) Diel biogeochemical processes and their effect on the aqueous chemistry of streams: a review. *Chem. Geol.* **283**, 3–17.

Pavlov V. K. and Pfirman S. L. (1995) Hydrographic structure and variability of the Kara Sea: Implications for pollutant distribution. *Deep-Sea Res. Pt II* **42**, 1369–1390.

Pearson E. J., Juggins S., Talbot H. M., Weckstrom J., Rosen P., Ryves D. B., Roberts S. J. and Schmidt R. (2011) A lacustrine GDGT-temperature calibration from the Scandinavian Arctic to Antarctic: renewed potential for the application of GDGT-paleothermometry in lakes. *Geochim. Cosmochim. Acta* **75**, 6225–6238.

Peterse F., Kim J.-H., Schouten S., Kristensen D. K., Koç N. and Sinninghe Damsté J. S. (2009) Constraints on the application of the MBT/CBT palaeothermometer at high latitude environments (Svalbard, Norway). *Org. Geochem.* **40**, 692–699.

Peterse F., Nicol G. W., Schouten S. and Sinninghe Damsté J. S. (2010) Influence of soil pH on the abundance and distribution of core and intact polar lipid-derived branched GDGTs in soil. *Org. Geochem.* **41**, 1171–1175.

Peterse F., van der Meer J., Schouten S., Weijers J. W. H., Fierer N., Jackson R. B., Kim J.-H. and Sinninghe Damsté J. S. (2012) Revised calibration of the MBT–CBT paleotemperature proxy based on branched tetraether membrane lipids in surface soils. *Geochim. Cosmochim. Acta* **96**, 215–229.

Pitcher A., Hopmans E. C., Schouten S. and Sinninghe Damsté J. S. (2009) Separation of core and intact polar archaeal tetraether lipids using silica columns: insights into living and fossil biomass contributions. *Org. Geochem.* **40**, 12–19.

Santruckova H., Bird M. I., Kalaschnikov Y. N., Grund M., Elhottova D., Simek M., Grigoryev S., Gleixner G., Arneth A., Schulze E. D. and Lloyd J. (2003) Microbial characteristics of soils on a latitudinal transect in Siberia. *Glob. Change Biol.* **9**, 1106–1117.

Schouten S., Huguet C., Hopmans E. C., Kienhuis M. V. M. and Sinninghe Damsté J. S. (2007) Analytical methodology for TEX86 paleothermometry by high-performance liquid chromatography/atmospheric pressure chemical ionization-mass spectrometry. *Anal. Chem.* **79**, 2940–2944.

Schouten S., Eldrett J., Greenwood D. R., Harding I., Baas M. and Sinninghe Damsté J. S. (2008) Onset of long-term cooling of Greenland near the Eocene–Oligocene boundary as revealed by branched tetraether lipids. *Geology* **36**, 147–150.

Schouten S., Hopmans E. C., van der Meer J., Mets A., Bard E., Bianchi T. S., Diefendorf A., Escala M., Freeman K. H., Furukawa Y., Huguet C., Ingalls A., Menot-Combes G., Nederbragt A. J., Oba M., Pearson A., Pearson E. J., Rosell-Mele A., Schaeffer P., Shah S. R., Shanahan T. M., Smith R. W., Smittenberg R., Talbot H. M., Uchida M., Van Mooy B.

A. S., Yamamoto M., Zhang Z. H. and Sinninghe Damsté J. S. () An interlaboratory study of TEX86 and BIT analysis using high-performance liquid chromatography–mass spectrometry. *Geochem. Geophys. Geosyst.* **10**, 1–13.

Schouten S., Hopmans E. C. and Sinninghe Damsté J. S. (2013) The organic geochemistry of glycerol dialkyl glycerol tetraether lipids: A review. *Org. Geochem.* **54**, 19–61.

Sinninghe Damsté J. S., Hopmans E. C., Pancost R. D., Schouten S. and Geenevasen J. A. J. (2000) Newly discovered non-isoprenoid glycerol dialkyl glycerol tetraether lipids in sediments. *Chem. Commun.* **17**, 1683–1684.

Sinninghe Damsté J. S., Schouten S., Hopmans E. C., van Duin A. C. T. and Geenevasen J. A. J. (2002) Crenarchaeol: the characteristic core glycerol dibiphytanyl glycerol tetraether membrane lipid of cosmopolitan pelagic crenarchaeota. *J. Lipid Res.* **43**, 1641–1651.

Sinninghe Damsté J. S., Ossebaar J., Abbas B., Schouten S. and Verschuren D. (2009) Fluxes and distribution of tetraether lipids in an equatorial African lake: constraints on the application of the TEX86 palaeothermometer and BIT index in lacustrine settings. *Geochim. Cosmochim. Acta* **73**, 4232–4249.

Smith L. C. and Pavelsky T. M. (2008) Estimation of river discharge, propagation speed, and hydraulic geometry from space: Lena River, Siberia: river discharge and hydraulic geometry. *Water Resour. Res.* **44**, W03427.

Sorokovikova L. M. (1997) Gaseous regime of the Yenisei River under present conditions. *Water Resour.* **24**, 80–83.

Stedmon C. A., Amon R. M. W., Rinehart A. J. and Walker S. A. (2011) The supply and characteristics of colored dissolved organic matter (CDOM) in the Arctic Ocean: Pan Arctic trends and differences. *Mar. Chem.* **124**, 108–118.

Stolbovoi V. I. S. and Sheremet B. (2002) General soil characteristics. In Stolbovoi V. and McCallum I., (eds.), *Land Resources of Russia CD-ROM*. International Institute for Applied Systems Analysis and the Russian Academy of Science, Laxenburg, Austria.

Sun Q., Chu G. Q., Liu M. M., Xie M. M., Li S. Q., Ling Y. A., Wang X. H., Shi L. M., Jia G. D. and Lu H. Y. (2011) Distributions and temperature dependence of branched glycerol dialkyl glycerol tetraethers in recent lacustrine sediments from China and Nepal. *J. Geophys. Res. Biogeosci.* **116**. Available at: WOS:000286760300003.

Telang S. A., Pocklington R., Naidu A. S., Romankevich E. A., Gitelson I. I. and Gladyshev M. I. (1991) Carbon and mineral transport in major North American, Russian, and Siberian rivers: the St Lawrence, the Mackenzie, the Yukon, the Arctic Alaskan rivers, the Arctic Basin rivers, and the Yenisei. In Degens E.T., Kempe S. and Richey J.E. (eds.), *Biogeochemistry of Major World Rivers SCOPE*. John Wiley & Sons. pp. 75–104.

Tierney J. E. and Russell J. M. (2009) Distributions of branched GDGTs in a tropical lake system: Implications for lacustrine application of the MBT/CBT paleoproxy. *Org. Geochem.* **40**, 1032–1036.

Tierney J. E., Russell J. M., Eggermont H., Hopmans E. C., Verschuren D. and Sinninghe Damsté J. S. (2010) Environmental controls on branched tetraether lipid distributions in tropical East African lake sediments. *Geochim. Cosmochim. Acta* **74**, 4902–4918.

Tierney J. E., Schouten S., Pitcher A., Hopmans E. C. and Sinninghe Damsté J. S. (2012) Core and intact polar glycerol dialkyl glycerol tetraethers (GDGTs) in Sand Pond, Warwick, Rhode Island (USA): insights into the origin of lacustrine GDGTs. *Geochim. Cosmochim. Acta* **77**, 561–581.

Van Dongen B. E., Semiletov I., Weijers J. W. H. and Gustafsson Ö. (2008) Contrasting lipid biomarker composition of terrestrial organic matter exported from across the Eurasian Arctic by the five great Russian Arctic rivers. *Global Biogeochem. Cycle* **GB22**, 1011.

Verschuren D., Sinninghe Damsté J. S., Moernaut J., Kristen I., Blauw M., Fagot M. and Haug G. H. (2009) Half-precessional dynamics of monsoon rainfall near the East African Equator. *Nature* **462**, 637–641.

Wang H., Liu W., Zhang C. L., Wang Z., Wang J., Liu Z. and Dong H. (2012) Distribution of glycerol dialkyl glycerol tetraethers in surface sediments of Lake Qinghai and surrounding soil. *Org. Geochem.* **47**, 78–87.

Weijers J. W. H., Schouten S., Hopmans E. C., Geenevasen J. A. J., David O. R. P., Coleman J. M., Pancost R. D. and Sinninghe Damsté J. S. (2006a) Membrane lipids of mesophilic anaerobic bacteria thriving in peats have typical archaeal traits. *Environ. Microbiol.* **8**, 648–657.

Weijers J. W. H., Schouten S., Spaargaren O. C. and Sinninghe Damsté J. S. (2006b) Occurrence and distribution of tetraether membrane lipids in soils: Implications for the use of the TEX86 proxy and the BIT index. *Org. Geochem.* **37**, 1680–1693.

Weijers J. W. H., Schouten S., van den Donker J. C., Hopmans E. C. and Sinninghe Damsté J. S. (2007) Environmental controls on bacterial tetraether membrane lipid distribution in soils. *Geochim. Cosmochim. Acta* **71**, 703–713.

White D. C., Davis W. M., Nickels J. S., King J. D. and Bobbie R. J. (1979) Determination of the sedimentary microbial biomass by extractible lipid phosphate. *Oecologia* **40**, 51–62.

Yang G., Zhang C. L., Xie S., Chen Z., Gao M., Ge Z. and Yang Z. (2013) Microbial glycerol dialkyl glycerol tetraethers from river water and soil near the three Gorges Dam on the Yangtze River. *Org. Geochem.* **56**, 40–50.

Zech R., Gao L., Tarozo R. and Huang Y. (2012) Branched glycerol dialkyl glycerol tetraethers in Pleistocene loess-paleosol sequences: three case studies. *Org. Geochem.* **53**, 38–44.

Zell C., Kim J.-H., Moreira-Turcq P., Abril G., Hopmans E. C., Bonnet M.-P., Sobrinho R. L. and Sinninghe Damsté J. S. (2013) Disentangling the origins of branched tetraether lipids and crenarchaeol in the lower Amazon river: implications for GDGT-based proxies. *Limnol. Oceanogr.* **58**, 343–353.

Zhu C., Weijers J. W. H., Wagner T., Pan J. M., Chen J. F. and Pancost R. D. (2011) Sources and distributions of tetraether lipids in surface sediments across a large river-dominated continental margin. *Org. Geochem.* **42**, 376–386.

Associate editor: Elizabeth Ann Canuel